Structure and Stability of Hereditary Spherocytosis Mutants of the Cytosolic Domain of the Erythrocyte Anion Exchanger 1 Protein†

Susan P. Bustos and Reinhart A. F. Reithmeier*

Department of Biochemistry, University of Toronto, 1 King's College Circle, Medical Sciences Building, Room 5216, Toronto, Ontario M5S 1A8, Canada

Received August 24, 2005; Revised Manuscript Received November 16, 2005

ABSTRACT: Anion exchanger 1 (AE1, Band 3) is the predominant membrane protein of erythrocytes. Its 52 kDa C-terminal domain functions as a chloride−bicarbonate exchanger, while its 43 kDa N-terminal cytosolic domain (cdb3) anchors the cytoskeleton to the membrane. Several proteins bind to cdb3, including protein 4.2, a cytoskeletal protein. Three mutations in cdb3 are associated with hereditary spherocytosis (HS) and decreased levels of protein 4.2 in erythrocytes. In this study, these cdb3 mutants (E40K, G130R, and P327R) were expressed in and purified from *Escherichia coli*. Sedimentation experiments showed that the wild-type and mutant proteins are dimers. No difference in secondary structure between mutant and wild-type proteins was detected using circular dichroism (CD) analysis. The wild-type and mutant proteins underwent similar pH-dependent conformational changes when monitored by intrinsic tryptophan fluorescence. Urea denaturation of proteins monitored by intrinsic fluorescence showed no significant differences in the sensitivity of the proteins to this chemical denaturant. Thermal denaturation monitored by CD and by calorimetry revealed that only the P327R mutant had a significantly lower midpoint of transition (∼5 °C) than the wild-type protein, suggesting a modest decrease in stability. The results show that the HS mutant cdb3 proteins do not differ to any great extent in structure from the wild-type protein, suggesting that the HS mutations may directly affect protein 4.2 binding.

Hereditary spherocytosis (HS)[1] is a common hemolytic anemia characterized by osmotically fragile spherocytes that are selectively trapped and destroyed in the spleen. The clinical severity of the disease ranges from asymptomatic to compensated hemolysis and to severe hemolytic anemia requiring frequent transfusions. This variation in severity is due to the different molecular defects that lead to HS and to bone marrow compensation (*1*).

HS is caused by defects in erythrocyte proteins that are involved in the major interaction between the erythrocyte membrane and the cytoskeleton: spectrin, ankyrin, protein 4.2, and the anion exchanger 1 (AE1, Band 3) protein. Because of the weakened interactions between the membrane and the cytoskeleton, membrane blebbing occurs, the surface area-to-volume ratio of the cell decreases, and the cell becomes spherical and unstable. Approximately 20% of HS cases are due to mutations in AE1 (*2*).

AE1 is the major integral membrane glycoprotein of red blood cells comprising ∼25% of the total membrane protein and is present at a level of $\sim 1.2 \times 10^6$ copies per cell (*3*). Human AE1 is a 95 kDa protein which consists of 911 amino acids arranged in two distinct domains, an N-terminal cytosolic domain and a C-terminal membrane domain, that can function independently of each other. The 52 kDa C-terminal membrane domain is defined as the region from Gly-361 to Val-911 since mild proteolytic cleavage at Lys-360 with trypsin separates the cytosolic domain from the membrane domain (*4*). The C-terminal domain spans the membrane up to 12 times and carries out the electroneutral exchange of bicarbonate and chloride, thereby increasing the carbon dioxide carrying capacity of the blood (*5*). The 43 kDa N-terminal cytosolic domain (cdb3) encompasses residues Met-1−Lys-360. Its N-terminal region is extraordinarily acidic, and the N-terminal methionine is N-acetylated (*6*, *7*). The N-terminal domain binds to cytoskeletal proteins, including protein 4.2 and ankyrin, as well as glycolytic enzymes, deoxyhemoglobin, and hemichromes (*8*).

Erythrocyte cdb3 partially purified from proteolyzed red blood cells yields fragments 43 and 41 kDa in size, and separation of these fragments has not been achieved (*8*). To obtain pure cdb3 for crystallization, the protein has been expressed in *Escherichia coli* and the purified recombinant protein compared to the cdb3 released from red blood cells by proteolysis (*9*). Both forms of the protein were shown to

† Supported by a grant from the Canadian Institutes of Health Research. S.P.B. was supported by a Graduate Student Fellowship from the Canadian Blood Services.

* To whom correspondence should be addressed: 1 King's College Circle, Room 5216 Medical Sciences Building, Department of Biochemistry, University of Toronto, Toronto, ON M5S 1A8, Canada. Telephone: (416) 978-7739. Fax: (416) 978-8548. E-mail: r.reithmeier@utoronto.ca.

[1] Abbreviations: A_{600}, absorbance at 600 nm; AE1, anion exchanger 1; CD, circular dichroism; cdb3, cytosolic domain of Band 3; C_m, midpoint of the urea unfolding transition; DSC, differential scanning calorimeter or calorimetry; DTT, dithiothreitol; ER, endoplasmic reticulum; ESI-TOF, electrospray ionization time-of-flight; HEK, human embryonic kidney; HS, hereditary spherocytosis; IPTG, isopropyl β-D-thiogalactopyranoside; LB, Luria Bertani; MW_{app}, apparent molecular weight; MW_{seq}, sequence molecular weight; Ni−NTA, nickel−nitrilotriacetic acid; PCR, polymerase chain reaction; PMSF, phenylmethanesulfonyl fluoride; SDS−PAGE, sodium dodecyl sulfate−polyacrylamide gel electrophoresis; T_m, midpoint of the thermal denaturation transition; WT, wild-type.

10.1021/bi051692c CCC: $33.50
Published on Web 12/24/2005

have the same secondary structure and pH-dependent conformational change. The recombinant protein was also shown to exist as a soluble stable dimer with the same Stokes radius as native cdb3. Both forms of cdb3 also had essentially identical affinities for ankyrin. The only structural difference detected was the absence of N-acetylation of the recombinant protein that is present in erythrocyte cdb3. Apart from this modification, no other structural or functional differences between recombinant and erythrocyte cdb3 could be detected, allowing the recombinant protein to be used for crystallization and other biochemical studies.

Mutations in both the membrane and cytosolic domains of AE1 can result in HS. Seven missense mutations in AE1 that are located in the membrane domain and are associated with HS were examined previously in our lab. The mutant proteins exhibited impaired binding to an inhibitor affinity matrix (SITS Affi-Gel), which indicated they had non-native structures and may be misfolded. They also exhibited defective cellular trafficking from the ER to the plasma membrane in HEK-293 cells and retained the normal protein in the ER by heterodimer formation (*10*). The retention of misfolded mutant AE1 in the ER would result in a decrease in the amount of AE1 at the membrane of red blood cells. This would account for the weakened interactions between the membrane and cytoskeleton and the resulting membrane instability.

Three cytosolic domain mutations associated with HS occur with a normal amount of AE1 at the red cell membrane. These mutations are E40K (Band 3 Montefiore), G130R (Band 3 Fukuoka), and P327R (Band 3 Tuscaloosa). Interestingly, although the red cell content of AE1 is normal, these three mutations are associated with 88% (homozygous state), 55% (homozygous state), and 29% (heterozygous state) decreases in the amount of protein 4.2 in the red cell, respectively (*11*−*13*). The stability of protein 4.2 may depend on its assembly with AE1 during biosynthesis or during its 120 day life in the mature red blood cell.

The crystal structure of the cytosolic domain of human AE1 expressed in *E. coli* was determined by X-ray diffraction, and the domain was found to exist as a symmetric dimer (*14*). Each monomer is made up of a globular peripheral protein binding domain and a C-terminal dimerization arm, which interacts with the arm of the other subunit to form the dimer. The structure of the cytosolic domain is shown in Figure 1 with the location of the G130R and P327R HS mutations indicated. The E40K mutation is located in the structurally unresolved extreme N-terminus of the cytosolic domain so is not expected to have a major effect on the structure of cdb3, but introduction of a positive charge here may affect protein 4.2 binding. The G130R mutation is located in a prominent α-helix of the peripheral protein binding domain. On the basis of the crystal structure, the side chain extends away from the body of the protein, so arginine here may disrupt protein 4.2 binding. The P327R mutation is located at the N-terminus of the major α-helix of the dimerization domain. Arginine could allow continuation of the helix but may affect dimerization (*15*). All three of these mutations result in the incorporation of a positively charged amino acid into a domain with predominantly negative surface potential, which could have consequences in binding of protein 4.2 where introduction of a positive charge may perturb the protein−protein interactions.

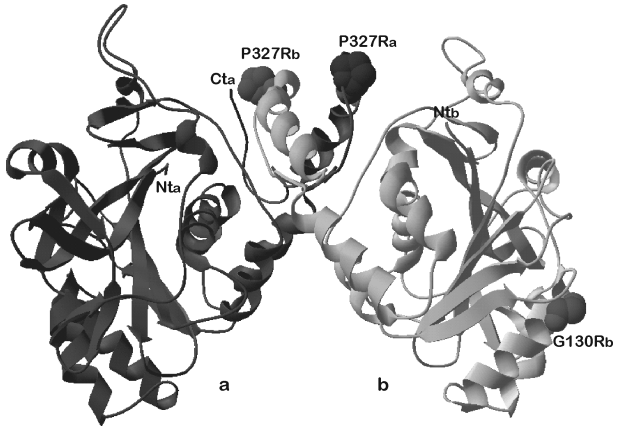

FIGURE 1: Crystal structure of the cytosolic domain of human AE1 (cdb3). The symmetric dimer of cdb3 was crystallized and its structure determined by X-ray diffraction (*14*). One subunit is colored dark gray (a) and the other subunit light gray (b). The locations of the HS G130R and P327R mutations are indicated on the structure. The location of the E40K mutation is not displayed in the structure since residues 1−54 cannot be resolved in the crystal structure. Abbreviations: a, subunit a; b, subunit b; Nt, N-terminal; Ct, C-terminal.

Band 3 Memphis I is another cytosolic domain mutant of AE1 where lysine at position 56 is substituted with glutamic acid (K56E). This polymorphism is widespread and is not associated with HS, but is characterized by the reduced electrophoretic mobility of the protein on SDS−PAGE (*16*). The resulting protein is thought to have an elongated cytosolic domain, and it has been proposed that the Memphis I variant is the evolutionarily older form (*17*). It is interesting that a mutation that occurs so close to an HS mutation (E40K) in the extreme N-terminus of the protein does not itself cause the disease. The K56 residue is the first resolvable residue in the cdb3 crystal structure. It is located just before the first β-strand of the protein, which lies within the center of the peripheral protein binding domain and may not be accessible to protein binding as is the E40 residue.

The Band 3 Tuscaloosa mutation (P327R) has been found to occur in cis with the Memphis I mutation (K56E) in one individual with HS (*12*). Since Band 3 Memphis I is an asymptomatic variant that represents a widespread polymorphism found in hematologically normal subjects (*17*), it is unlikely that this mutation contributes to the phenotype seen in this patient. Also, in the crystal structure (*14*), the P327 and K56 residues are quite far apart (29 Å) and are not expected to interact. However, with only one patient found to possess the P327R mutation, it is unclear whether the P327R mutation alone or in combination with the Memphis I mutation produces the HS phenotype.

The goal of this work was to express and purify the three HS mutant cdb3 proteins (E40K, G130R, and P327R) and to compare their structure and stability to those of the wild-type cdb3 protein. The Memphis I cdb3 protein was included in the study as an asymptomatic mutant control. The stability of the Band 3 Tuscaloosa double mutant (P327R/K56E) was also examined to determine the role of the Memphis I background on this HS mutant. We hypothesize that three HS cytosolic domain mutations in AE1 affect the folding and/or the stability of cdb3, which would result in impaired binding of protein 4.2 and lead to its deficiency in the red blood cells of patients with these mutations.

MATERIALS AND METHODS

Materials. The following is a list of materials used and their suppliers: pcDNA3 vector (Invitrogen, San Diego, CA); QuikChange site-directed mutagenesis kit (Stratagene, La Jolla, CA); mutagenic primers (ACGT Corp., Toronto, ON); pETBlue-1 vector and Tuner(DE3)pLacI *E. coli* competent cells (Novagen, Madison, WI); growth media for *E. coli* (BD, Sparks, MD); chloramphenicol and carbenicillin (Sigma, St. Louis, MO); isopropyl β-D-thiogalactopyranoside (Bioshop, Burlington, ON); Ni−NTA agarose resin (QIAGEN, Germantown, MD); and Sequanal grade urea (Pierce, Rockford, IL).

Plasmid Construction and Mutagenesis. cdb3 from Met-1 to Ser-356 was amplified by PCR from full-length human AE1 located on the pcDNA3 vector and cloned into the pETBlue-1 expression vector, which contains an IPTG-inducible T7*lacO* promoter (*18*). The reverse primer included DNA encoding six histidine residues which are located at the C-terminus of the protein to provide a hexahistidine tag for purification. The HS mutants and K56E variant were constructed using the QuikChange system with complementary mutagenic primers, and the mutations were confirmed by sequencing by ACGT Corp.

Protein Expression and Purification. All protein expression was performed in *E. coli* strain Tuner(DE3)pLacI. This strain of *E. coli* is a derivative of the BL21 strain, but has a mutation in the lac permease gene which allows uniform entry of IPTG into all cells and inhibits basal level protein expression. pETBlue-1 vectors were expressed in Tuner(DE3)pLacI which contains the gene for T7 RNA polymerase under the control of the IPTG-inducible *lacUV5* promoter (*19*). Cells were grown at 37 °C in LB medium containing both carbenicillin (50 μg/mL) and chloramphenicol (34 μg/mL) until the cell density reached an A_{600} of 0.6. Protein expression was induced with 1 mM IPTG; then cells were grown for an additional 4 h at 37 °C, and cell density reached an A_{600} of 1.3. Cells were harvested by centrifugation (4400*g* for 30 min) and solubilized in 80 mL of lysis buffer [50 mM sodium phosphate, 300 mM sodium chloride, 5 mM imidazole, 0.2% β-mercaptoethanol, and 0.2% Triton X-100 (pH 8.0)] per liter of cell culture containing the following protease inhibitors: 0.70 μg/mL pepstatin, 2.0 μg/mL aprotinin, 4.3 μg/mL leupeptin, and 0.28 μg/mL PMSF. Solubilized cells were allowed to sit on ice for 30 min after addition of lysozyme to a final concentration of 1 mg/mL, followed by sonication at 40% duty for 2 min on ice. Purification was carried out by a batch procedure at 4 °C using 1 mL of Ni−NTA agarose resin (QIAGEN) per 80 mL of cell lysate. Resin was washed twice with 10 mL of wash buffer [50 mM sodium phosphate, 300 mM sodium chloride, 20 mM imidazole, and 0.2% β-mercaptoethanol (pH 8.0)]. Proteins were eluted three times with 1 mL of elution buffer [50 mM sodium phosphate, 300 mM sodium chloride, 250 mM imidazole, and 0.2% β-mercaptoethanol (pH 8.0)]. Protein solutions were applied to pre-equilibrated PD-10 gel filtration columns (Amersham Biosciences) for the purpose of buffer exchange into 10 mM ammonium bicarbonate and subsequent lyophilization. Proteins were lyophilized overnight and were stored at −20 °C. Protein purity was determined to be >95% by Coomassie staining of samples following SDS−PAGE. Protein concentrations were determined by the Bio-Rad protein assay based on the Bradford assay. Protein samples were subjected to mass spectroscopy on an ESI-TOF instrument for molecular weight analysis to verify the identity of the proteins. A cysteine-less protein in which both cysteines of cdb3 were mutated to alanine (C201A/C317A) was also submitted for analysis.

Analytical Ultracentrifugation. Sedimentation equilibrium experiments were performed at 20 °C on an Optima XL-A/XL-I analytical ultracentrifuge (Beckman Instruments, Palo Alto, CA) using an AN50-Ti rotor, quartz windows, and standard six-sector charcoal-filled Epon centerpieces. Samples were centrifuged at 18000*g*, 32000*g*, and 50000*g* for 27 h at each speed to ensure equilibrium was reached before absorbance measurements were taken. Global analysis of the data was performed using XL-A/XL-I data analysis software (Origin version 4.1) from Beckman Instruments. Sedimentation was performed on three different concentrations of each protein (0.32, 0.64, and 1.29 mg/mL) in 10 mM sodium phosphate and 50 mM sodium chloride (pH 7.5). Proteins had been freshly purified using Ni−NTA resin and buffer-exchanged into sedimentation buffer using PD-10 columns without freeze-drying.

Circular Dichroism. Freeze-dried cdb3 proteins were dissolved in 10 mM sodium phosphate, 50 mM sodium fluoride, and 1 mM DTT (pH 7.0) (*20*). Circular dichroism spectra from 190 to 260 nm with a 1 nm data pitch were recorded on a Jasco J-810 spectropolarimeter using a final protein concentration of 0.3 mg/mL cdb3 in a 1 mm path length cell at 24 °C. Deconvolution of spectra was done using the CDPro software package (*21*) for determination of secondary structure fractions. For temperature denaturation, samples were heated from 30 to 86 °C with a 2 °C data pitch at a scan rate of 2 °C/min and ellipticity was measured at 208 nm. Thermal denaturation data were fit to a standard equation by nonlinear least-squares regression (using SigmaPlot 2004 version 9.0) assuming a two-state transition for a dimeric species. T_m is the temperature at the transition midpoint of thermal unfolding. Experiments were repeated using at least three different preparations of purified protein.

pH Dependence of the Intrinsic Fluorescence. Stock solutions of cdb3 proteins were made by dissolving proteins in 50 mM sodium phosphate, 50 mM sodium borate, 70 mM sodium chloride, and 1 mM DTT (pH 7.0) (*22*). The stock protein solution was diluted 50 times into the same buffer preadjusted to the desired pH to a final protein concentration of 0.17 mg/mL. Samples were equilibrated for at least 2 h at room temperature prior to measurement. In all fluorescence experiments, the intrinsic fluorescence of the proteins was monitored using a Fluorolog FL3-22 fluorescence spectrophotometer at 24 °C. The excitation wavelength was 290 nm, and the fluorescence emission was measured from 300 to 420 nm for each sample at each pH. Experiments were repeated using three different preparations of purified protein.

Calorimetry. cdb3 proteins were dissolved in 10 mM sodium phosphate and 50 mM sodium chloride (pH 7.5) to a final concentration of 1.3 mg/mL. Heat capacity measurements were obtained on a Microcal VP-DSC differential scanning calorimeter. Samples were heated from 25 to 90 °C at a rate of 1.5 °C/min. Temperature denaturation data

Table 1: Effects of HS Mutations on the Structure and Stability of cdb3 Protein

cdb3 protein	MW_{app}/MW_{seq}	α-helix (%)	T_m (°C) (CD)	T_m (°C) (calorimetry)	C_m (M)
WT	1.981[a]	28.5[b] ± 3.3	69.0[c] ± 2.2	66.2[e] ± 1.5	4.79[d] ± 0.31
E40K	2.026	28.3 ± 1.7	68.4[b] ± 0.3	64.9[b] ± 0.3	4.73 ± 0.13
G130R	1.950	27.9 ± 1.5	68.7[b] ± 0.4	65.5[b] ± 0.3	4.85 ± 0.09
P327R	1.921	28.3 ± 2.6	64.0[b] ± 0.4	61.5[b] ± 0.2	4.56 ± 0.20
K56E	2.011	26.7 ± 4.4	67.7[d] ± 1.5	66.5[f] ± 2.0	4.60[b] ± 0.15

[a] Data from nine sedimentation equilibrium measurements (three different protein concentrations run at three different speeds) were globally fit to the single-ideal species model to obtain the apparent molecular weight (MW_{app}). [b] Values are averages of measurements obtained from three different preparations of purified protein. [c] Values are averages of measurements obtained from nine different preparations of purified protein. [d] Values are averages of measurements obtained from six different preparations of purified protein. [e] Values are averages of measurements obtained from 12 different preparations of purified protein. [f] Values are averages of measurements obtained from seven different preparations of purified protein. For CD and calorimetry measurements, T_m is the temperature at the midpoint of the thermal denaturation transition. C_m is the concentration of urea at the midpoint of the urea-induced unfolding transition.

were fit to the following standard equation:

$$C_p(T) = [K_A(T)\Delta H_{mA}{}^*\Delta H_{mA}]/\{[1 + K_A(T)]^2 RT^2\} + ...$$

using the Origin 7.0 data analysis software which employs the Marquardt−Levenberg algorithm for least-squares regressions. Experiments were repeated using at least three different preparations of purified protein.

Urea Denaturation Measured by Intrinsic Fluorescence. Stock solutions of cdb3 proteins were made by dissolving proteins in 50 mM sodium phosphate, 50 mM sodium borate, 70 mM sodium chloride, and 1 mM DTT (pH 7.0). The stock protein solution was diluted 50 times into the same buffer preadjusted to the desired urea concentration to a final concentration of 0.17 mg/mL. Samples were equilibrated in denaturant at room temperature for 2 h prior to measurement. The excitation wavelength was 290 nm, and the fluorescence emission was measured from 300 to 420 nm for each protein at each urea concentration at 24 °C. Urea denaturation data were fit to a standard equation by nonlinear least-squares regression (using SigmaPlot 2004 version 9.0) assuming a two-state transition of a dimeric species. C_m is the urea concentration at the midpoint of the unfolding transition. Experiments were repeated using six different preparations of purified protein, except for experiments with the K56E mutant which were repeated using three protein preparations.

Limited Tryptic Digestion. Proteins were dissolved in 50 mM sodium phosphate, 50 mM sodium borate, and 70 mM sodium chloride (pH 7.0). Trypsin dissolved in the same buffer was added to each sample to a final concentration of 6.5 μg/mL (final protein concentration of 0.3 mg/mL). The digestion reaction was allowed to proceed for 5 min at room temperature and was stopped by the addition of an equal volume of 2× sample buffer containing SDS and β-mercaptoethanol. Samples were run on SDS−PAGE and were detected by Coomassie Blue staining. Relative sizes of the protein bands were determined by loading of Protein Molecular Weight Markers (Fermentas, Burlington, ON) on the gel.

RESULTS

Expression and Purification of cdb3 and cdb3 HS Variants in E. coli. The region of cdb3 encompassing amino acids 1−356 of the protein was subcloned from full-length wild-type AE1 cDNA on the pcDNA3 vector into a pETBlue-1 expression vector and expressed in *E. coli* Tuner(DE3)pLacI cells as described in Materials and Methods. These residues extend from the amino terminus of AE1 to the last residue visible in the crystal structure, followed directly by a His_6 tag. The purification of the His_6-tagged wild-type cdb3 and cdb3 carrying the E40K, G130R, and P327R mutations was carried out by Ni^{2+} affinity chromatography. This purification method yielded more than 20 mg of protein per liter of cell culture of more than 95% purity as determined by SDS gel electrophoresis. The cdb3 proteins ran as monomers of approximately 41 kDa on SDS−PAGE (data not shown). Mass spectroscopy analysis revealed expected molecular masses for all proteins with additional molecular masses of either 76 or 152 Da on all of the proteins (data not shown). These additions were not seen with the cysteine-less (C201A/C317A) mutant. The extra molecular masses were likely due to a β-mercaptoethanol adduct on one (+76 Da) or both (+152 Da) of the cysteines.

Sedimentation Equilibrium of Wild-Type and HS Mutant cdb3 Proteins. Sedimentation equilibrium analyses were carried out to determine whether the HS mutations affected the oligomeric structure of the cdb3 protein. Purified wild-type cdb3 has been shown to exist as a dimer (*9*, *14*, *22*, *23*). The predicted sequence molecular mass of wild-type cdb3 with a His_6 tag is 40 866 Da. Sedimentation equilibrium centrifugation was performed on wild-type, HS, and K56E mutant cdb3 proteins using different protein concentrations and rotor speeds, and the data were fit to a single-ideal species model. The analysis gave apparent molecular weights that were twice that of the sequence molecular weights which indicated that the wild-type, HS, and K56E mutant proteins existed as stable dimers in solution. No evidence of concentration dependence of the molecular weight values was observed over a range from 0.32 to 1.29 mg/mL. The ratios of the apparent molecular weight to the sequence molecular weight determined by sedimentation equilibrium analysis are listed in Table 1, and a representative sedimentation plot of wild-type cdb3 run at 32000*g* is shown in Figure 2.

Secondary Structure Analysis of Wild-Type and HS Mutant cdb3 Proteins. Circular dichroism (CD) analysis was carried out to determine whether the HS mutations affect the secondary structure of the cdb3 protein. The CD spectrum of wild-type cdb3 has been shown to exhibit a negative extreme at 208 nm and a shoulder at 223 nm typical of an α-helical structure-containing protein (*22*). Figure 3 shows the CD spectra obtained from the wild-type and HS mutant cdb3 proteins. The spectra from this study display the same characteristics as those obtained from native cdb3, and those of the mutant cdb3 proteins overlap with the spectrum from

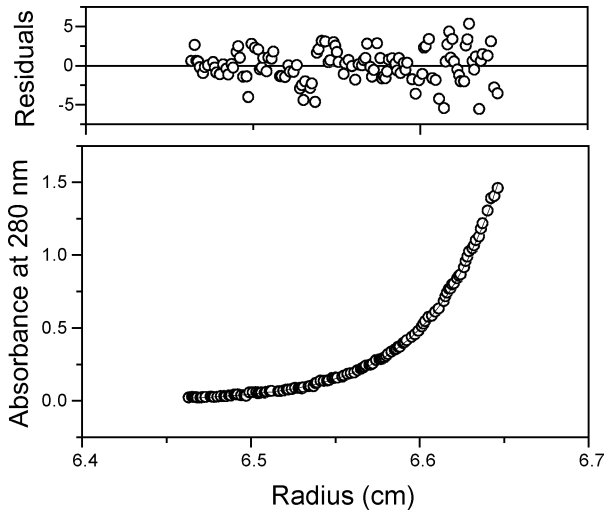

FIGURE 2: Sedimentation equilibrium of wild-type cdb3. Absorbance is plotted as a function of radius, and the residuals from fitting the data to a single-ideal species model are shown. The experiment was performed at 20 °C with a rotor speed of 32000*g* for 27 h. The protein concentration was 0.64 mg/mL, and the protein was in 10 mM sodium phosphate and 50 mM sodium chloride (pH 7.5).

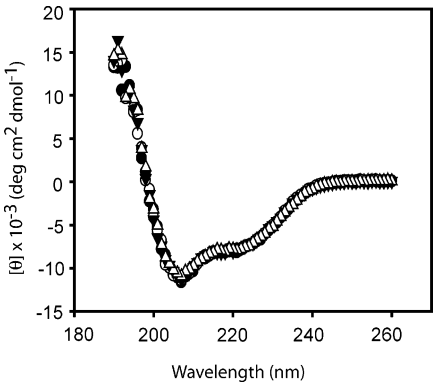

FIGURE 3: Circular dichroism spectra of wild-type cdb3 and HS mutants. Purified proteins were dissolved in 10 mM sodium phosphate, 50 mM sodium fluoride, and 1 mM DTT (pH 7.0) and scanned at 24 °C in a 1 mm cell in a Jasco J-810 spectropolarimeter. The final concentration of all proteins was 0.3 mg/mL: wild-type (●), E40K (○), G130R (▼), and P327R (△). Spectra are expressed as the mean residue ellipticity.

the wild-type protein. Similar spectra were obtained for the Memphis I mutant protein (data not shown). The helical content of the cdb3 protein obtained from the crystal structure was 26% (*14*). The helical contents of wild-type, HS, and K56E mutant cdb3 proteins obtained by deconvolution of the CD spectra shown in Table 1 are similar to that found in the crystal structure. The HS mutations did not result in any major change in the secondary structure of cdb3.

Effect of pH on the Intrinsic Fluorescence of the Wild-Type and HS Mutant cdb3 Proteins. cdb3 has been shown to undergo a reversible pH-dependent conformational change that is characterized by a dramatic increase in the intrinsic tryptophan fluorescence and an increase in the Stokes radius without a change in secondary structure at alkaline pH (*9*). A hydrogen bond between W105 of one subunit and D316 of the other subunit that is present in the lower-pH conformation is broken at neutral pH (*24*). At alkaline pH, the conformation of cdb3 changes extensively as the peripheral protein binding domain moves away from the dimerization arm. In the study presented here, intrinsic

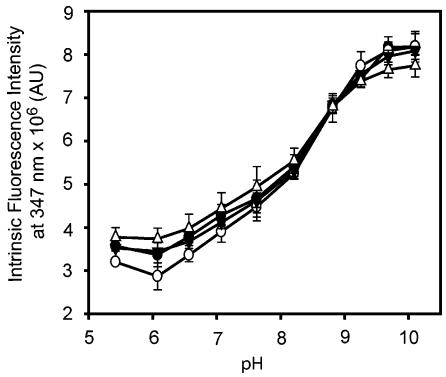

FIGURE 4: Intrinsic fluorescence intensity of wild-type cdb3 and HS mutants as a function of pH. Purified proteins were dissolved in 50 mM sodium phosphate, 50 mM sodium borate, 70 mM sodium chloride, and 1 mM DTT (pH 7.0) to a stock concentration of 10 mg/mL. All samples were filtered through a 0.22 μm syringe filter, and 6 μL of each stock protein solution was added to 294 μL (50× dilution) of the same buffer preadjusted to the desired pH. The final concentration was 0.17 mg/mL for all proteins, and the actual pH was measured in each reaction tube using a pH meter. The intrinsic fluorescence intensities at 347 nm of the wild-type (●), E40K (○), G130R (▼), and P327R (△) are plotted as a function of pH.

tryptophan fluorescence was measured over a pH range to determine whether the HS mutations caused a difference in the pH-dependent conformational change of the cdb3 protein. Figure 4 shows the intrinsic fluorescence emission intensity at 347 nm of the wild-type and HS mutant cdb3 proteins as a function of pH. The proteins exhibited a similar increase in fluorescence intensity, representing a dequenching of tryptophans, and an increase in peak wavelength (red shift) at alkaline pH (data not shown), indicating that the tryptophans were exposed to a more polar environment. There was a moderate increase in fluorescence emission intensity between pH 5 and 8, followed by a more dramatic increase between pH 8 and 10 for all samples. The results indicate that the wild-type and mutant proteins undergo similar two-stage pH-dependent conformational changes.

Thermal Denaturation of Wild-Type and HS Mutant cdb3 Proteins by Circular Dichroism. The HS mutations did not appear to affect the folded structure or oligomeric state of the cdb3 protein, but the mutations may affect the stability of this domain. Thermal denaturation using circular dichroism was performed to determine if the HS mutants lowered the stability of the cdb3 protein. Figure 5 shows the results of thermal denaturation as monitored by CD at 208 nm at pH 7.0. The midpoints of the thermal denaturation transitions (T_m) for each protein are listed in Table 1. The wild-type protein had a T_m of 69.0 °C. The P327R cdb3 protein had a T_m that was 5 °C lower than that of the wild-type. The E40K, G130R, and Memphis I (data not shown) cdb3 proteins did not have significantly lower melting temperatures. The P327R mutant appears to be less stable than the other proteins, while the E40K and G130R mutants have stabilities similar to that of the wild-type protein. The thermal denaturation of all the proteins was irreversible as determined by rescanning of cooled samples after heating to 86 °C.

Thermal Denaturation of Wild-Type and HS Mutant cdb3 Proteins by Calorimetry. Thermal denaturation was also performed using differential scanning calorimetry (DSC). The

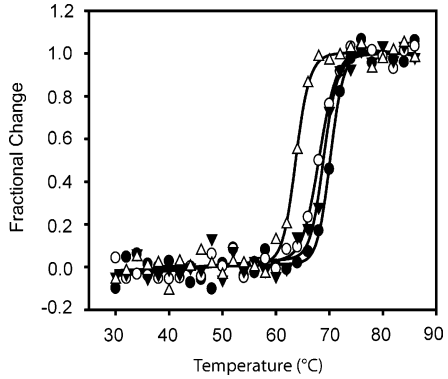

FIGURE 5: Thermal denaturation of wild-type cdb3 and HS mutants monitored by CD. Purified wild-type and HS mutant cdb3 proteins were dissolved in 10 mM sodium phosphate, 50 mM sodium fluoride, and 1 mM DTT (pH 7.0) for CD measurements. The final concentration of the proteins was 0.3 mg/mL: wild-type (●), E40K (○), G130R (▼), and P327R (△). Ellipticity was measured at 208 nm as the temperature was increased from 30 to 86 °C in 2 °C increments.

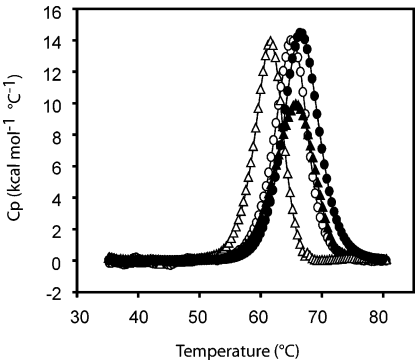

FIGURE 6: Thermal denaturation of wild-type cdb3 and HS mutants by differential scanning calorimetry. The proteins were dissolved in 10 mM sodium phosphate and 50 mM sodium chloride (pH 7.5) at a final protein concentration of 1.3 mg/mL: wild-type (●), E40K (○), G130R (▼), and P327R (△). The heat capacity was measured as the temperature was increased from 35 to 80 °C, and the baseline-subtracted values are presented. No transition was observed after the samples were cooled and reheated.

melting temperature of the wild-type cdb3 protein measured by differential scanning calorimetry has been shown to be pH-dependent and was reported to be 67 °C at pH 7.51 (*22*). Figure 6 shows the results of the baseline-subtracted DSC scans. The melting temperatures for each protein at pH 7.5 obtained using DSC are listed in Table 1. The wild-type protein had a T_m of 66.2 °C, which is in agreement with results of previous studies. The P327R cdb3 protein had a T_m that was 5 °C lower than that of the wild type. The E40K, G130R, and K56E cdb3 proteins had melting temperatures similar to that of the wild-type. The P327R/K56E double mutant protein had a T_m (62.2 °C) that was not significantly different from that of the P327R single mutant (61.5 °C). Although the absolute melting temperatures differ slightly from those obtained from the CD thermal denaturation experiments, the relative values are similar. The thermal denaturation of all the proteins was irreversible since rescanning cooled samples after heating to 90 °C yielded scans with no transition. The thermal denaturation studies show that only the P327R mutation results in very modest destabilization of the cdb3.

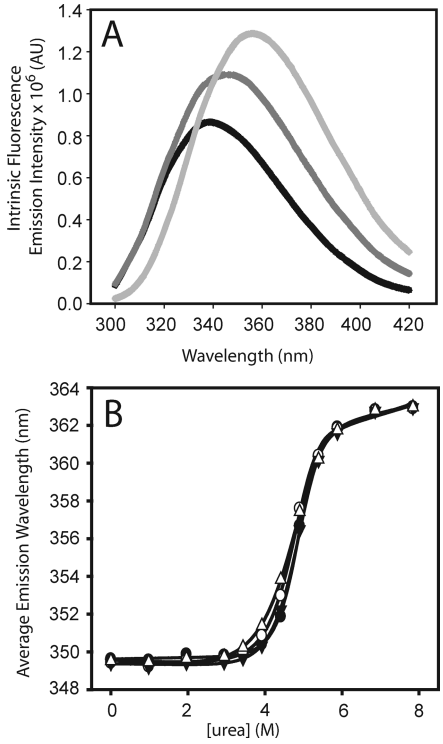

FIGURE 7: Urea denaturation of wild-type and HS mutant cdb3 proteins. Purified wild-type and HS mutant cdb3 proteins were dissolved in 50 mM sodium phosphate, 50 mM sodium borate, 70 mM sodium chloride, and 1 mM DTT (pH 7.0) to a stock concentration of 10 mg/mL. All samples were filtered through a 0.22 μm syringe filter, and 6 μL of each stock protein solution was added to 294 μL (50× dilution) of the same buffer preadjusted to the desired urea concentration. The final concentration was ~0.17 mg/mL for all proteins. Samples were equilibrated for 2 h before measurements were taken. The intrinsic fluorescence emission was measured from 300 to 420 nm (λ_{ex} = 290 nm) for each protein at each urea concentration. (A) Intrinsic fluorescence emission spectra of wild-type cdb3 are plotted for three urea concentrations: 0 (black line), 5 (dark gray line), and 8 M (light gray line). (B) The average emission wavelength of the wild type (●), E40K (○), G130R (▼), and P327R (△) was calculated from each spectrum and plotted as a function of urea concentration.

Urea Denaturation of Wild-Type and HS Mutant cdb3 Proteins. Urea denaturation was also used to study the stability of the cdb3 proteins. Urea is a chaotropic agent that causes proteins to denature, and proteins with decreased stabilities will unfold at lower urea concentrations (*25*). The concentration dependence of urea denaturation of the wild-type cdb3 protein at pH 6.0 has been shown to cause an increase in intrinsic fluorescence intensity as the urea concentration increased, with the midpoint of the transition at ~5 M urea (*24*). In this study, urea denaturation of the wild-type and HS mutant cdb3 proteins at pH 7.0 resulted in an increase in the intrinsic fluorescence intensity as tryptophans became unquenched, and an increase in peak wavelength as protein unfolding exposed tryptophans to a more polar environment. Figure 7 shows emission intensity spectra for wild-type cdb3 at different urea concentrations and the increase in average emission wavelength as a function of urea concentration for wild-type and HS mutant proteins. The transition midpoints (C_m) for each protein are listed in Table 1. The C_m values for the mutant proteins were similar to that of the wild-type protein, and their differences were not statistically significant. Dilution of cdb3 proteins in 8

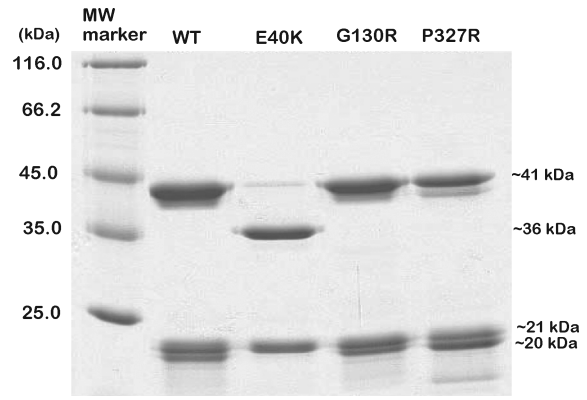

FIGURE 8: Trypsin digestion of wild-type and HS mutant cdb3 proteins. Purified wild-type and HS mutant cdb3 proteins were dissolved in 50 mM sodium phosphate, 50 mM sodium borate, and 70 mM sodium chloride (pH 7.0) and incubated with trypsin dissolved in the same buffer. Digestion proceeded for 5 min at room temperature, and the reaction was stopped by addition of an equal volume of 2× sample buffer. The final cdb3 protein and trypsin concentrations were 0.3 mg/mL and 6.5 μg/mL, respectively. Digested proteins were run on SDS−PAGE and detected by Coomassie Blue staining.

M urea into buffer to give a final urea concentration of less than 1 M did not result in refolding of cdb3 (data not shown), indicating that the unfolding was irreversible.

Limited Tryptic Digestion of Wild-Type and HS Mutant cdb3 Proteins. Limited tryptic digestion of cdb3 proteins was used to measure the folded structures of the proteins. Trypsin cleaves after lysine and arginine residues in areas of a folded protein that are accessible to the protease. Regions of the protein where cleavage sites are buried within the folded structure of the protein will not be readily cleaved. Wild-type and HS mutant cdb3 proteins (0.3 mg/mL) were incubated with trypsin (6.5 μg/mL) for 5 min at room temperature, and the reaction was stopped by addition of an equal volume of sample buffer containing SDS and β-mercaptoethanol. Samples were run on SDS−PAGE and visualized with Coomassie Blue staining as seen in Figure 8. Cleavage patterns of the G130R and P327R mutants were similar to the wild-type pattern. The full-length 41 kDa cdb3 protein was present along with the appearance of two smaller bands of approximately 21 and 20 kDa, perhaps representing the two fragments obtained from cleavage at one site of the protein by trypsin. The E40K protein gave a different cleavage pattern with a prominent band of ~36 kDa and the 21 kDa band. The E40K mutant introduces a new trypsin cleavage site at lysine 40, and cleavage at this new site would account for the appearance of the 36 kDa band, which is approximately 40 residues smaller than the full-length protein. A Western blot using an antibody against the N-terminus of cdb3 confirmed that the 20 kDa band was derived from the N-terminal region of the protein (data not shown). The 36 kDa band from the E40K digest was not detected since its first 40 residues had been cleaved off. The 21 kDa band for all of the proteins was not detected by the N-terminal antibody, indicating that this fragment was derived from the C-terminal region of the protein. The Memphis I mutant protein removes a potential trypsin cleavage site (K56E) in the protein, but the wild-type and HS mutant proteins examined still have a lysine at position 56. No fragment corresponding to cleavage at this site was observed for any of the proteins. Trypsin was unable to cleave at this position, indicating that it was not accessible to the protease which is consistent with this residue's buried location in the crystal structure. The protease digestion results indicate that the HS mutations did not induce gross misfolding of cdb3, consistent with the cooperative unfolding seen by thermal or chemical denaturation. The results also indicate that the region around residue 40 is very accessible, while residue 56 is not.

DISCUSSION

HS mutations in the cytosolic domain of AE1 were found to cause no major changes in the structure of the domain. The mutants of cdb3 retained the dimeric structure of the protein as seen in sedimentation equilibrium experiments. Even the P327R mutation which is located at the N-terminus of an α-helix in the dimerization arm did not interfere with the formation of a dimer by the protein. The mutants also retained the normal secondary structure of the protein as seen in circular dichroism experiments. The mutations may not be expected to cause a major disruption in the secondary structure since the E40K mutation is located in a structurally unresolved region, and the G130R residue points away from the protein and into the solvent. Arginine at position 327, instead of proline, could allow continuation of the helix that follows it, and no detectable change in the helical content of this mutant was observed. All three mutants underwent pH-dependent conformational changes similar to that of the wild-type protein as monitored by intrinsic tryptophan fluorescence, indicating that their folded structures are similar. This pH-dependent behavior is important physiologically since binding of glycolytic enzymes, deoxyhemoglobin, and cytoskeletal proteins to AE1 in the red cell membrane is very sensitive to pH.

The E40K mutant displayed a different pattern of limited tryptic digestion since it introduced a new trypsin cleavage site at residue 40. This indicates that the residue at position 40 is accessible to trypsin and therefore is exposed to the solvent. Since there was no cleavage at the site of the Memphis I mutation, lysine 56, this indicates that this residue is not accessible to trypsin and therefore not exposed to the solvent in the folded structure. Even though residues 40 and 56 are only 16 residues apart in the primary sequence of the protein, their environments in the tertiary structure of the protein are quite different. Residue E40's lack of resolution in the crystal structure also provides evidence of its surface accessibility, while K56 is one of the first residues to be resolved. It is more likely that a surface residue, such as E40, is involved with protein−protein interactions versus one that is less surface-exposed, such as K56. This could be why a mutation at the E40 site is associated with disease while a mutation at the K56 site is tolerated. Since trypsin was unable to cleave at lysine 56 in the wild-type and HS mutant proteins, this provides evidence for the similarity in their folded structures.

The P327R mutant resulted in modest destabilization of cdb3 as seen in thermal denaturation experiments. Even though the P327R mutation did not cause any major structural changes in the protein, it did affect its stability, however slightly. Interestingly, the stability of the double mutant, P327R/K56E, was not significantly different from

that of the single P327R mutant, and the stability of the K56E mutant was similar to that of the wild-type protein. This provides evidence for the first time that the underlying cause for the HS phenotype in the patient with this double mutant is the P327R mutation, and not K56E.

Destabilization of HS mutant proteins was not seen in the experiments in which urea was used as the denaturant, not even with the P327R mutant. The lack of destabilization seen with the P327R mutant could be due to different modes of unfolding by thermal and chemical denaturation. Intrinsic fluorescence spectroscopy, the technique used to probe for unfolding in the urea unfolding experiments, is a measure of the environment of the four tryptophans in the protein. From these experiments, there does not appear to be much difference in these environments overall between the HS mutant proteins and the wild-type version during unfolding by urea.

The results show that the loss of binding of protein 4.2 to cdb3 is not the result of a major structural change in cdb3, but may be the result of changes at the binding interface due to the introduction of positive charges which occurs with each of these HS mutations. The asymptomatic polymorphism K56E also retains the major structural features of the protein and has stability similar to that of the wild-type protein. Since residue 56 is not exposed to the solvent, unlike residue 40, there may be no consequences regarding protein binding, and hence no association between this mutation and HS.

This is the first study to show that the molecular basis of HS associated with these three HS mutations is not caused by a structural deformity in the cytosolic domain of AE1, which is in keeping with the normal amount of these mutant proteins at the red cell membrane of these patients. This supports the idea that the phenotype is likely caused by perturbation at the binding interface between cdb3 and protein 4.2 at the specific sites of mutation. The HS mutation sites are not clustered together in the folded structure of cdb3 as seen in the crystal structure, but are located far from each other, which indicates that the cdb3−protein 4.2 binding interface may be large. The loss of binding of protein 4.2 to the cytosolic domain of AE1 may result in destabilization of protein 4.2. To test this hypothesis and to further characterize the molecular basis of this red cell membrane defect, future studies will include testing the effect of the HS mutations on the binding of protein 4.2 to AE1 in *in vitro* binding assays and in transfected cells.

ACKNOWLEDGMENT

We thank Jing Li for assistance in the construction of the HS mutant AE1 vectors. We also thank Walid Houry for the use of the fluorescence and circular dichroism spectrometers, David Clarke for the use of the differential scanning calorimeter, and Avi Chakrabartty and Rongmin Zhao for the sedimentation equilibrium analyses.

REFERENCES

1. Iolascon, A., Miraglia del Giudice, E., Perrotta, S., Alloisio, N., Morle, L., and Delaunay, J. (1998) Hereditary spherocytosis: From clinical to molecular defects, *Haematologica 83*, 240−257.
2. Lux, S. E., and Palek, J. (1995) Disorders of the red cell membrane, in *Blood: Principles and Practice of Hematology* (Handin, R. I., Lux, S. E., and Stossel, T. P., Eds.) pp 1701, Lippincott, Philadelphia.
3. Fairbanks, G., Steck, T. L., and Wallach, D. F. (1971) Electrophoretic analysis of the major polypeptides of the human erythrocyte membrane, *Biochemistry 10*, 2606−2617.
4. Lepke, S., and Passow, H. (1976) Effects of incorporated trypsin on anion exchange and membrane proteins in human red blood cell ghosts, *Biochim. Biophys. Acta 455*, 353−370.
5. Jennings, M. L. (1989) Structure and function of the red blood cell anion exchange protein, *Prog. Clin. Biol. Res. 292*, 327−338.
6. Kaul, R. K., Murthy, S. N., Reddy, A. G., Steck, T. L., and Kohler, H. (1983) Amino acid sequence of the Nα-terminal 201 residues of human erythrocyte membrane band 3, *J. Biol. Chem. 258*, 7981−7990.
7. Drickamer, L. K. (1978) Orientation of the band 3 polypeptide from human erythrocyte membranes. Identification of NH_2-terminal sequence and site of carbohydrate attachment, *J. Biol. Chem. 253*, 7242−7248.
8. Low, P. S. (1986) Structure and function of the cytoplasmic domain of band 3: Center of erythrocyte membrane-peripheral protein interactions, *Biochim. Biophys. Acta 864*, 145−167.
9. Wang, C. C., Badylak, J. A., Lux, S. E., Moriyama, R., Dixon, J. E., and Low, P. S. (1992) Expression, purification, and characterization of the functional dimeric cytoplasmic domain of human erythrocyte band 3 in *Escherichia coli*, *Protein Sci. 1*, 1206−1214.
10. Quilty, J. A., and Reithmeier, R. A. (2000) Trafficking and folding defects in hereditary spherocytosis mutants of the human red cell anion exchanger, *Traffic 1*, 987−998.
11. Inoue, T., Kanzaki, A., Kaku, M., Yawata, A., Takezono, M., Okamoto, N., Wada, H., Sugihara, T., Yamada, O., Katayama, Y., Nagata, N., and Yawata, Y. (1998) Homozygous missense mutation (band 3 Fukuoka: G130R): A mild form of hereditary spherocytosis with near-normal band 3 content and minimal changes of membrane ultrastructure despite moderate protein 4.2 deficiency, *Br. J. Haematol. 102*, 932−939.
12. Jarolim, P., Palek, J., Rubin, H. L., Prchal, J. T., Korsgren, C., and Cohen, C. M. (1992) Band 3 Tuscaloosa: Pro327→Arg327 substitution in the cytoplasmic domain of erythrocyte band 3 protein associated with spherocytic hemolytic anemia and partial deficiency of protein 4.2, *Blood 80*, 523−529.
13. Rybicki, A. C., Qiu, J. J., Musto, S., Rosen, N. L., Nagel, R. L., and Schwartz, R. S. (1993) Human erythrocyte protein 4.2 deficiency associated with hemolytic anemia and a homozygous 40 glutamic acid→lysine substitution in the cytoplasmic domain of band 3 (band 3 Montefiore), *Blood 81*, 2155−2165.
14. Zhang, D., Kiyatkin, A., Bolin, J. T., and Low, P. S. (2000) Crystallographic structure and functional interpretation of the cytoplasmic domain of erythrocyte membrane band 3, *Blood 96*, 2925−2933.
15. Low, P. S., Zhang, D., and Bolin, J. T. (2001) Localization of mutations leading to altered cell shape and anion transport in the crystal structure of the cytoplasmic domain of band 3, *Blood Cells Mol. Dis. 27*, 81−84.
16. Yannoukakos, D., Vasseur, C., Driancourt, C., Blouquit, Y., Delaunay, J., Wajcman, H., and Bursaux, E. (1991) Human erythrocyte band 3 polymorphism (band 3 Memphis): Characterization of the structural modification (Lys 56→Glu) by protein chemistry methods, *Blood 78*, 1117−1120.
17. Jarolim, P., Rubin, H. L., Zhai, S., Sahr, K. E., Liu, S. C., Mueller, T. J., and Palek, J. (1992) Band 3 Memphis: A widespread polymorphism with abnormal electrophoretic mobility of erythrocyte band 3 protein caused by substitution AAG→GAG (Lys→Glu) in codon 56, *Blood 80*, 1592−1598.
18. Giordano, T. J., Deuschle, U., Bujard, H., and McAllister, W. T. (1989) Regulation of coliphage T3 and T7 RNA polymerases by the lac repressor-operator system, *Gene 84*, 209−219.
19. Studier, F. W., and Moffatt, B. A. (1986) Use of bacteriophage T7 RNA polymerase to direct selective high-level expression of cloned genes, *J. Mol. Biol. 189*, 113−130.
20. Johnson, W. C., Jr. (1990) Protein secondary structure and circular dichroism: A practical guide, *Proteins 7*, 205−214.
21. Sreerama, N., and Woody, R. W. (2000) Estimation of protein secondary structure from circular dichroism spectra: Comparison of CONTIN, SELCON, and CDSSTR methods with an expanded reference set, *Anal. Biochem. 287*, 252−260.

22. Appell, K. C., and Low, P. S. (1981) Partial structural characterization of the cytoplasmic domain of the erythrocyte membrane protein, band 3, *J. Biol. Chem. 256*, 11104−11111.
23. Colfen, H., Harding, S. E., Boulter, J. M., and Watts, A. (1996) Hydrodynamic examination of the dimeric cytoplasmic domain of the human erythrocyte anion transporter, band 3, *Biophys. J. 71*, 1611−1615.
24. Zhou, J., and Low, P. S. (2001) Characterization of the reversible conformational equilibrium in the cytoplasmic domain of human erythrocyte membrane band 3, *J. Biol. Chem. 276*, 38147−38151.
25. Pace, C. N. (1986) Determination and analysis of urea and guanidine hydrochloride denaturation curves, *Methods Enzymol. 131*, 266−280.

BI051692C